Assessment of thin-walled cladding tube mechanical properties by segmented expanding Mandrel test

Karl-Fredrik Nilsson
Institute for Energy and Transport, Joint Research Centre, EC, The Netherlands

Abstract

This paper presents the principles of the segmented expanding mandrel test for thin-walled cladding tubes, which can be used as a basic material characterisation test to determine stress-strain curves and ductility or as a test to simulate mechanical pellet-cladding interaction. The paper discusses the strengths and weaknesses of the test method and it illustrates how the test can be used to simulate hydride reorientations in zirconium claddings and quantify how hydride reorientation affects ductility.

Introduction

A number of mechanical tests for thin-walled cladding tubes for nuclear fuel have been proposed such as ring-compression test, ring-tensile test, burst test, four-point bend tests and different mandrel tests [1-3]. The main purpose of a mechanical test is material characterisation, but simulation of representative loadings such as mechanical pellet-cladding interaction could also be a main objective. A material characterisation test should be as simple as possible to analyse and the deformation of the specimen should preferably evolve in a stable manner also under softening or defect growth. A test with axisymmetric displacement controlled loading would be ideal. A test to simulate pellet-cladding interaction should include the key interaction features. In this paper we will explore the segmented expanding cone-mandrel (ECM) test both as a material characterisation test and as a test to simulate the mechanical pellet-clad interaction. We will illustrate the application by investigating the ductility of zirconium alloys with re-oriented hydrides.

Description of the ECM test

The segmented expanded cone-mandrel (ECM) test was proposed in the eighties [4]. Figure 1a shows the principles of our test set-up [5][6] which consists of a cone, segments and the tube specimen. The set of segments is manufactured from a cylindrical body with outer radius equal to the inner radius of the tube to be tested. A conical volume with the same angle as the cone is removed from the central part of the cylinder. The cylinder is then cut into equal sized segments. When the cone is displaced vertically by a specific value,u_z, a corresponding radial displacement, $u_r = \tan(\frac{\theta}{2}) \cdot u_z$, is imposed on the segments and the inner surface of the tube. The segments do not carry any hoop stress and have a very small deformation. The tube will be subjected to a periodic but controlled radial displacement from the segments. At the segment edges more complex stress and strain concentrations occur that depend strongly on the friction between the segments and the cladding tube. As a component test it is desirable that the stress variations induced by the

segments are representative for mechanical fuel-cladding interaction whereas for a material characterisation test one would like to minimise them. Different loadings can be obtained by controlling the number of segments and the friction coefficient. The deformation becomes more axi-symmetric by increasing the number of segments and by reduced friction between the tube and the segments. A tube with segments and cone ready for testing is shown in Figures 1b and 1c after testing with significant deformation. The designed prototype for the experiment consists of a lower cylindrical block, a cone with angle 20° and sets of segments. The segments and cone were made from STAVAX, which is a very hard and wear resistant material. The height and outer diameter of the cylinder from which the segments are made are 9.7 mm and 9.2 mm respectively. The diameter of the cylindrical hole at the bottom is 2.8 mm and at the upper end it is 6.2 mm to fit the cone. The lower block has a hole with a diameter suitable to allow enough travel for the cone to move down into it, whilst still providing a sufficient support for the assembly of segments and tube with pure sliding. The vertical displacement and the reaction force are recorded during loading and the change in diameter is measured by a transverse extensometer. The test can be performed under load or displacement control. The contact surfaces in the examples below were sprayed with teflon to minimise friction.

Figure 1:
a) Schematic illustration of the principles for the cone mandrel test before loading and with 5% and 50% applied strain
b) loaded specimen with extensometer for strain measurement
c) tested tube at large deformation with cone and segments

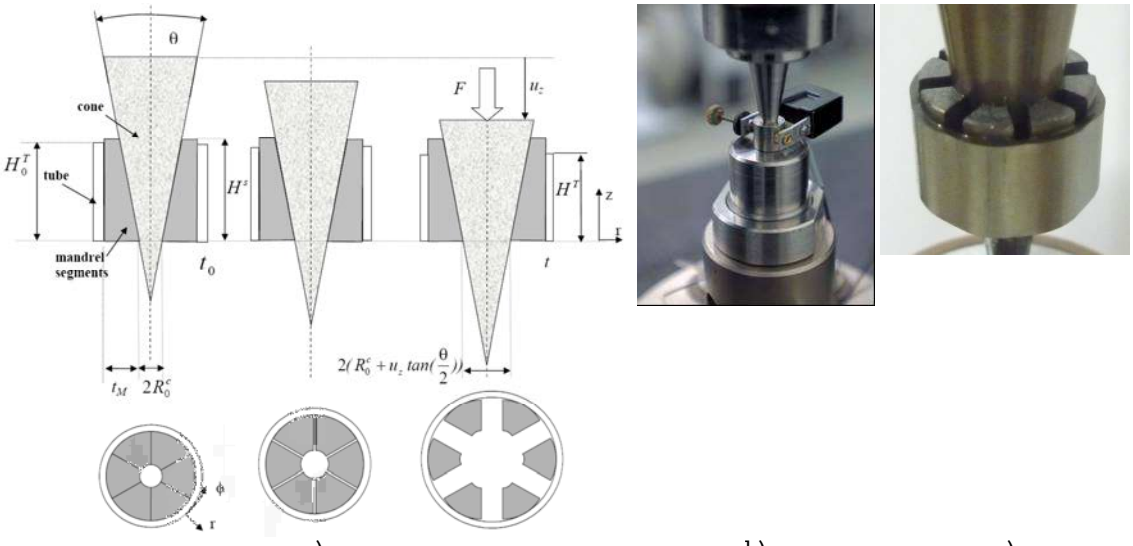

a) b) c)

Basic assessment of the SEM test

Stress-strain curve and axisymmetric model

Figure 2a shows the measured reaction forces versus the normalised radial displacement for six different tests. The first number in the legend (6, 8, 10 or 12) indicates the number of segments and the second number the sequence number of the test. The difference between the curves could stem from variation in the tensile properties between the tested tubes, or from variability of the test method itself. For instance it is obvious that the alignment of the segments between the tests and the friction between the different surfaces may vary between tests. Nevertheless the variation is not very large.

Figure 2: a) Measured reaction force vs. applied radial displacement; computed hoop stress-strain curve using the axi-symmetric analytical model and measured forces and displacement; b) Test 8-4 with different values of the friction coefficient but equal for all contact; c) all test tests with hard cone and friction coefficient = 0.04 d) friction coefficient 0.2 for all surfaces (None) and 0.2 for all but the surface indicated in the figure

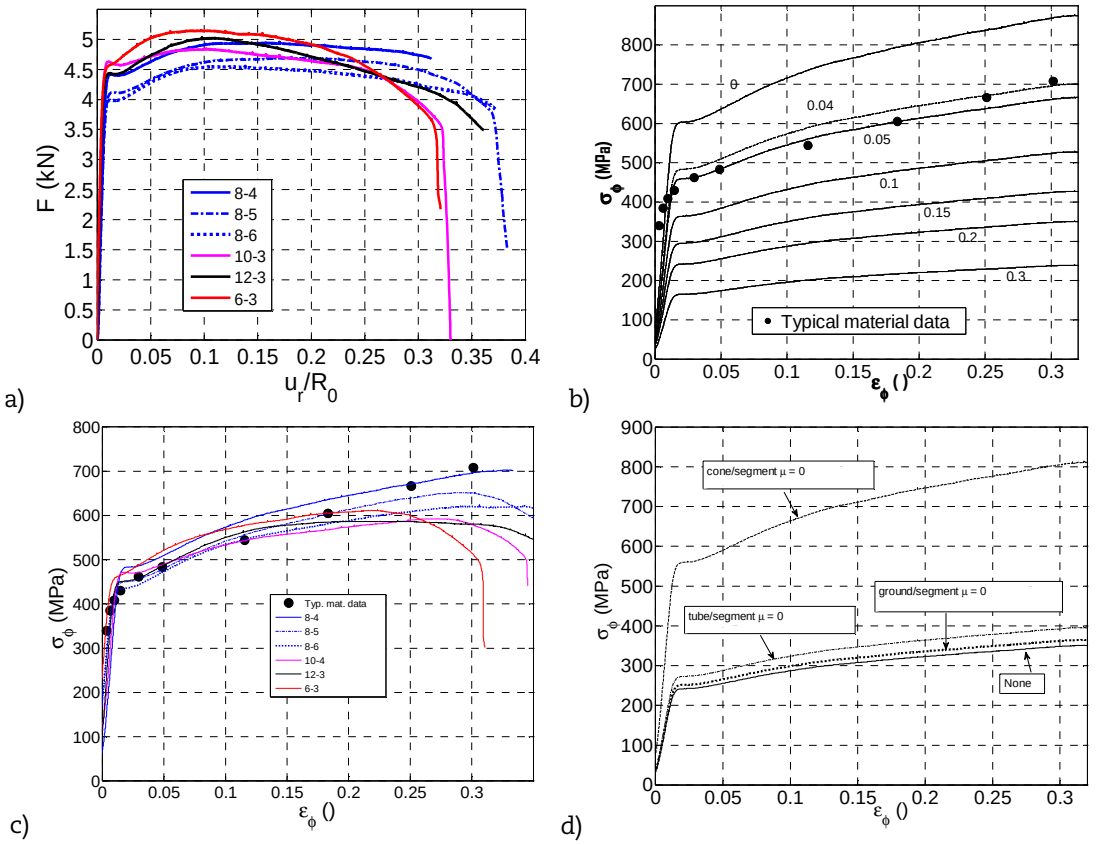

The test can be analysed with a semi-analytical model with the following assumptions: i) the deformation and loading are axisymmetric; ii) the cone and the segments are rigid but the segments do not carry any hoop stresses; iii) the contact model is a simple Coulumb friction; iv) the tube has constant hoop stress and is stress free in the axial direction, the radial stress is much smaller than the hoop stress and set to zero and there are no shear stresses; v) the material possesses orthotropic symmetry and plastic deformation is assumed to follow the Hill classic quadratic yield criterion. The equations are given in [5,6].

Figure 2b shows the computed stress-strain curves from the measured displacement and forces of test 8-4 for seven different values of the friction coefficient (0 to 0.3). The same friction coefficient is assumed between all contact surfaces and the material is assumed to be isotropic. The symbols in Figure 2b represent "typical data" from AREVA. A typical friction coefficient for teflon is 0.04 and we note that the computed curve with this value agrees quite well with the typical curve for this friction coefficient. In Figure 2c, the stress strain curves computed with a friction value of 0.04 are plotted for all six specimens. The curves diverge more at higher loads when localised plastic deformation develops in the opening between segments. Figure 2d shows the computed stress-strain curves from the data from test 8-4 for four different friction cases; one when the friction coefficient is 0.2 for each of the three contact surfaces and in the other cases it is 0.2 for two surfaces and 0 for one. The most important observation is that the friction has by far the largest effect for the cone/segment surface.

Effect of stress concentrations as segment edge

The edges of the expanding segments induce local stress concentrations on the cladding that qualitatively simulate the mechanical interaction between cracked fuel pellets and the cladding tube. This stress concentration decreases with increasing number of segments and gets stronger with increasing friction coefficient between segment and cladding tube. To assess this effect a 2D finite element analysis was performed for a half a segment. Figure 3 shows a typical FE-mesh set-up for the eight segment geometry. A controlled radial displacement is imposed on the inner surface of the segment, symmetry conditions are imposed along the lower boundary for segment and tube, whereas the upper boundary of the segment is traction free. Coulumb friction is assumed between tube and segment. Typical stress-strain curves for zircaloy-2 and STAVAX are used for tube and segment respectively.

Figure 3: Finite element and associated boundary conditions model for the 8-segment mandrel and tube

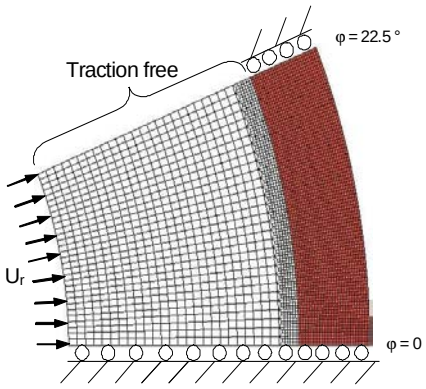

Figure 4: a) Hoop strain distributions along inner surface at 10% applied strain for different values of the friction coefficient with 8 segments; b) picture of undeformed tube and tube after large plastic deformation

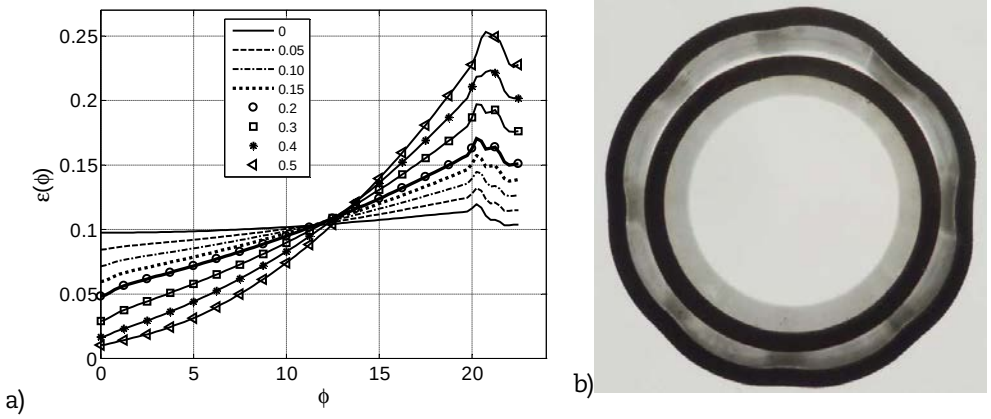

Figure 4a shows the computed hoop strain distributions along the inner surface of the tube at 10% applied strain for friction coefficients ranging from 0 to 0.5. The friction coefficient clearly influences the strain distribution. When the friction coefficient is zero the strain is almost axisymmetric. A friction coefficient of 0.5, which is typical for fresh fuel, gives a strain concentration factor of 2.5 at the inner surface. The deviation from axisymmetry increases with loading. Figure 4b shows an undeformed tube and a deformed tube loaded to 30% strain. The number of segments as well as the friction coefficient has a large impact on the variation in the tube's stress and strain distributions. The computed plastic effective strain distribution in the tube and cone at an applied engineering strain of 26% is plotted in Figures 5a and 5b for the case with 12 segments and zero friction coefficient and 8 segments

and friction coefficient 0.5 respectively. With friction the highest strain in the tube develops in the gap between the segments as clearly seen in Figure 5b. The stretched zones are also clearly seen in Figure 4b. Most of the overall plastic strain takes place in these regions with large deformation and low hardening of the material. This plastic strain localisation is the reason why the computed stress strain curves from the mandrel test as outlined above and illustrated in Figure 2 underestimates the plastic hardening at large strains. This effect increases with higher friction and fewer segments. It can also be noted that there is some plastic deformation at the inner segment corner. This may influence the load distribution since the curvature does not perfectly match the cone.

Figure 5: Computed plastic effective strain in segment and tube at applied radial displacement $\frac{u_r}{R} = 0.26$ a) 12 segments, μ = 0; b) 8 segments, μ = 0.5

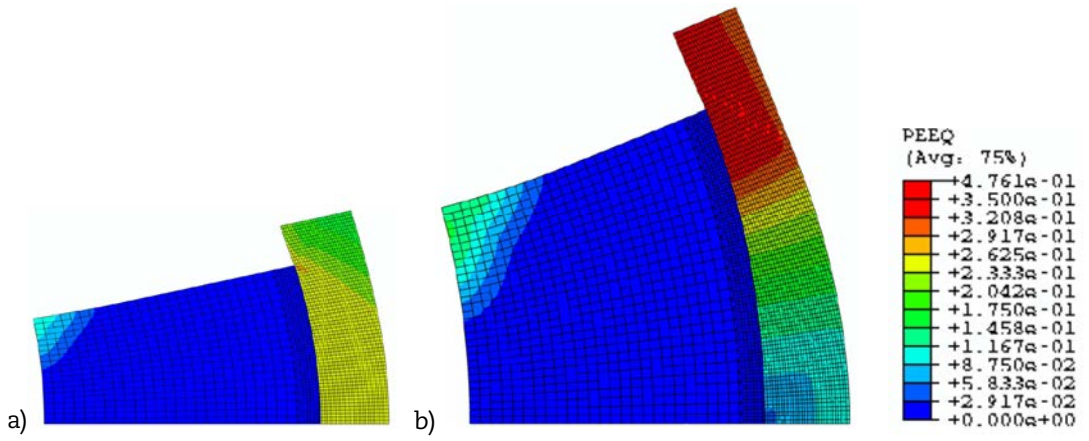

Applications of the SEM test

Hydride reorientation and embrittlement

Ziconium alloy fuel cladding pick up hydrogen from corrosion during reactor operation. When the spent fuel is cooled in water pools the hydrogen precipitates as hydrides with primarily circumferential orientation due to the texture of the cladding tube [7,8]. When the spent fuel is transferred from wet to dry storage the temperature increases to typically 400°C whereby the hydrides dissolve and the internal pressure in the cladding tubes increases to 6-16 MPa. When the cladding tubes are slowly cooled the hydrogen reprecipitates as radial hydrides due to the hoop stress [8]. At 400°C, the typical threshold value for hydride re-orientation is 60-100 MPa [8], which is attained from the internal pressure in the fuel claddings. The hydrides are much more brittle than the matrix material when the temperature is below 300°C. It has been observed that radial hydrides may drastically reduce the ductility of fuel claddings at low temperatures [7,8]. The ductility reduction is believed to be caused by a process where first hydrides fracture (typically at 1% strain) whereby the cladding tube becomes a multi-cracked material. Elasto-plastic fracture mechanics can then be applied to assess the ductility [9].

We used the mandrel test to first induce hydride re-orientation and subsequently to determine the ductility. To this end zircaloy-2 tubes that had been charged with nominal hydrogen content 100, 200 and 300 ppm were used. The re-orientation was achieved applying a constant load F and then heating up the ECM set-up in a furnace to a prescribed temperature, keeping the temperature constant for a specified and then slowly cooling the ECM set-up. Heat-up rate, cooling rate, hold time and number of cycles were varied between the tests.

The maximum temperature was set to slightly above 400°C and the constant load was selected to give a hoop stress of about 100 MPa. A typical load and temperature history is shown in Figure 6. Figure 7 shows micrographs of tested tubes with hydride content of 100,

200 and 300 ppm before and after reorientation. The re-orientation is obvious from the naked eye observation of the micrographs. The hydrides were mapped from micrographs with MATLAB based in-house image processing routines. Each individual hydride exceeding a threshold length was identified with respect to orientation, length and position.

Figure 6: Example of thermal and mechanical loading using SEM test to induce hydride re-orientation

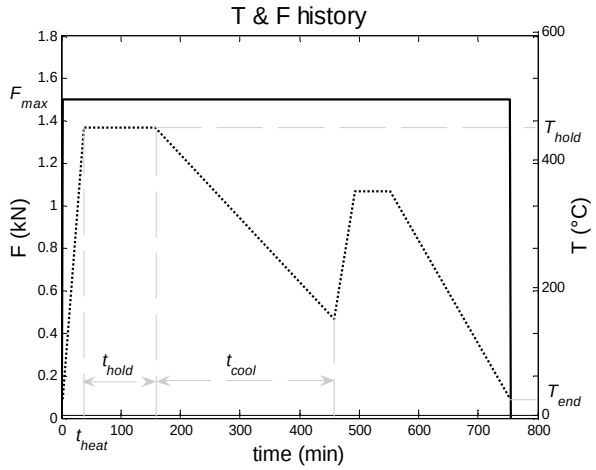

Figure 7: Examples of micrographs of tubes with nominally 100, 200 and 300 ppm hydrogen before and after re-orientation test. $Nrad_{45}^{X}$ and ε_{max} are the measured fraction of radial hydrides and the ductility for the specific specimens. X stands for the magnification of micrographs used for the hydride characterisation.

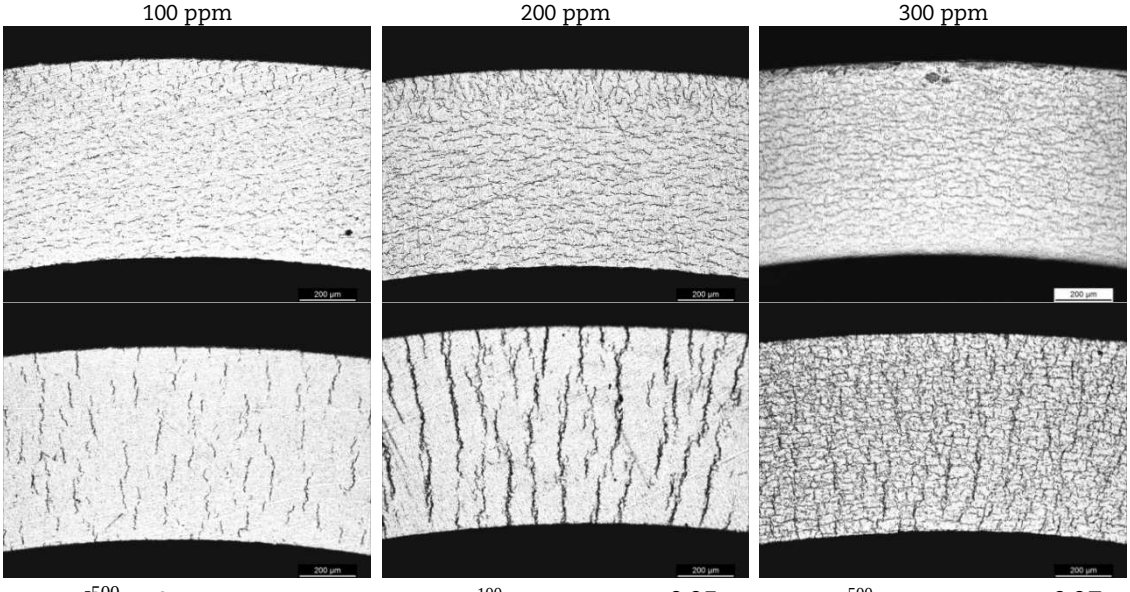

There is no agreed definition on hydride re-orientation. We consider hydrides that have an orientation larger than 45° from the circumferential direction as re-oriented. The re-orientation is then defined by the total length of radial hydrides divided by the length of all hydrides ($Nrad_{45} = \sum a_i(\varphi > 45°)/\sum a_i$) The re-orientation and other hydride parameters are derived from the image processed micrographs.

Tube specimens with different hydrogen content, as-received as well as re-oriented were subsequently tested by the SEM test in displacement controlled mode to measure the ductility. The ductility was defined as the hoop strain at which the specimen failed.

Figure 8 shows the measured ductility versus the content of radial hydride (measured radials hydride fraction multiplied with total hydrogen content). The symbols represent different levels of charged hydrogen. The observations from these tests are in line observations from spent fuel claddings: at these stresses and temperatures hydride re-orientation is likely; radial hydrides induce a significant loss of ductility; a smaller fraction of hydrides will be re-oriented at very high hydride levels resulting in a saturation of hydride embrittlement at high hydrogen levels.

Figure 8: Measured ductility vs. density of radial hydrides

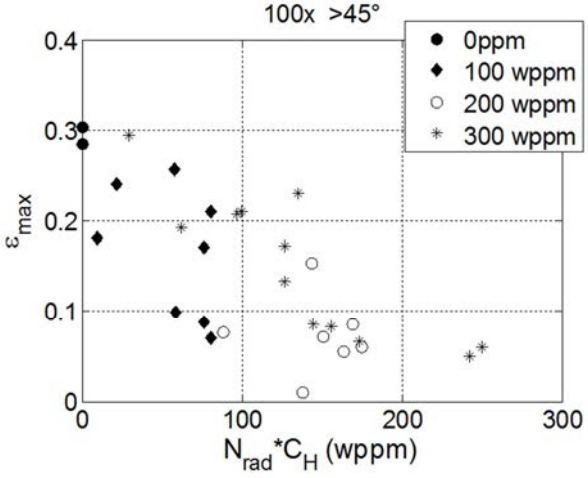

Corrosion loops

The AMALIA laboratory at JRC consists of corrosion loops with instrumented test sections for assessment of environmental assisted degradation. The present loops simulate conditions for boiling water, pressure water and super-critical water reactors and a loop with lead cooled reactors is under design. Conventional mechanical material testing systems produce the load on the specimen by using a moving pull rod, which is disadvantageous for testing in liquid or pressurized environments since pressure boundary feed-throughs cause problems with leakage and friction forces that are difficult to fully control. With bellows-based Pneumatic Loading Apparatus (PLA) it is possible to design test set-ups with no moving parts over the pressure boundary, i.e. a loading unit connected to the control unit via pressure lines and electrical feedback connectors only. Another advantage is that very accurate load control can be achieved. A PLA has therefore been developed by P. Moilanen [10] and implemented into the AMALIA lab for different specimen tests. A SEM loading device has now been designed for AMALIA based on the PLA. The on-line vertical displacement during the test will be recorded (bellows movement) and the change in diameter is measured indirectly by an LVDT displacement gauge. The device can then be used for stress corrosion cracking of cladding tubes under well controlled conditions. Figure 9 outlines the design.

Discussion

A number of proposed tests exists for thin-walled cladding tubes for material characterisation or safety assessment. The methods are complementary as they all have their strengths, drawbacks and limitations. Some strengths of the ECM-tests include: a small amount of material is needed and no specific specimen preparation is required; it is simple to perform; the analysis is simple provided the loading is reasonably axisymmetric; it is easy to combine with defect assessment; it can be performed as load

or displacement controlled; the test can be used both as a material characterisation test and simulation of mechanical fuel-cladding interaction. There are also a number of limitations. The most obvious one is the large influence of the friction between cone and segment and that the friction is difficult to control. Furthermore fraction my change as the surfaces may roughen with repeated tests. This problem can be mitigated by alternative materials for cone and segments that are very hard and have very fine surfaces. Another drawback is that the loading is uniaxial whereas the stress field is typically bi-axial. The test is difficult to perform in a hot cell since it is difficult to align the segments accurately using remote manipulators.

Figure 9: PLA test frame for segmented expanding mandrel

Conclusions

This paper has presented the principles of the segmented expanding mandrel test for thin-walled cladding tubes. As shown the test can be used as a mechanical characterisation test to determine the stress-strain curve in the hoop direction and the ductility. Moreover the expanding segments can simulate mechanical fuel cladding interaction from cracked fuel. The test is also relatively simple to perform in harsh environments using bellow based loading systems.

References

[1] Billone, M.C., Assessment of Current Test methods for Post-LOCA Cladding Behaviour, NUREG/CR-7139, ANL-11/52.

[2] Martin-Rengel, M.A. et al. (2012), Revisiting the method to obtain the mechanical properties of hydrided fuel cladding in the hoop direction, Journal of Nuclear Materials, 429, pp. 276-283.

[3] Yagnik, S.K. et al. (2008), “Round-Robin Testing of Fracture Toutgness Characteristics of Thin-Walled Tubing”, Journal of ASTM International, Vol. 5, Issue 2, pp 205-225.

[4] Nobrega, B.N., King, J.S., Was, G.S., Wisener, S.B. (1985), Improvements in the design and analysis of the segmented expanding mandrel test, Journal of Nuclear Materials, 131, 99-104.

[5] Nilsson, K.-F, O. Martin, C. Chenel-Ramos, J. Mendes (2011), Nuclear Engineering and Design, 241, 445-448.

[6] Nilsson, K.-F. and M. Negyesi (2011), Assessment of fuel cladding integrity by the segmented expanding mmandrel Test (SEM, Transactions SMiRT, 6-11 November 2011, New Dehli, India, Div-I: Paper ID# 65.

[7] Marshall, R.P. and M.R. Louthan (1963), Tensile properties of Zircaloy with Oriented Hydrides, ASM Transactions Quarterly, 56, pp. 693-700.

[8] Chu, H.C., S.K. Wu, R.C. Kuo (2008), Hydride re-orientation in Zircaloy-4 cladding, Journal of Nuclear Materials 373, pp. 319-327.

[9] Nilsson, K.-F., N. Jakšić and V. Vokál (2010), An elasto-plastic fracture mechanics based model for assessment of hydride embrittlement in zircaloy cladding tubes, Journal of Nuclear Materials., 396, pp. 71-85.

[10] Moilanen, P. et al., New applications of pneumatically powered testing equipment for extreme environments, in Baltica IX, Interantional Conference on Life Management and Maintenance for Power Plants, VTT Technology 106, ISBN 978-951-38-8026-2.